DE GRUYTER Journal of the Mechanical Behavior of Materials 2024; 33: 20240022

Research Article

C. Anil Kumar Reddy*, Pothamsetty Kasi V. Rao, Begori Venkatesh and Boggarapu Nageswara Rao

Influence of plasma nitriding on surface layer of M50NiL steel for bearing applications

https://doi.org/10.1515/jmbm-2024-0022
received August 10, 2024; accepted October 19, 2024

Abstract: Research on plasma nitriding was carried out on M50NiL bearing steel, subject to temperatures ranging from 460 to 560°C over periods from 4 to 40 h, while keeping the gas mixture at a steady ratio of $80H_2{:}20N_2$. To examine the phase structure and chemical composition of the plasma nitrided layer, techniques such as energy dispersive spectrometry (EDS) and X-ray diffraction (XRD) were utilized. The M50NiL steel sample heated to 550°C for 24 h was found to contain an unusually high amount of nitrogen, as per the EDS analysis. The majority of the nitrided layer's composition is made up of nitrogen-expended phases. Following XRD analysis, several peaks were identified, including α'-FeN, γ'-FeN, γ'-Fe_3N, α'-Fe, and γ'-Fe. The main objective of this research was to explore the impact of temperature on the microstructure, hardness, wear resistance, and corrosion resistance of the surface nitrided layers. The steel that underwent nitriding at 500°C for 4 h demonstrated a significantly higher surface hardness of 1,332 HV, with an additional increase in case depth by 62.00 µm. The findings suggest that both the duration and temperature of nitriding affect the depth of the plasma nitrided layer. The surface hardness of the plasma samples was found to be notably improved. The steel sample, PN 500, nitrided at 08 h, exhibited the highest wear resistance among the nitride samples. The wear resistance of the samples was shown to be significantly enhanced. Potentiodynamic tests were conducted to assess the corrosion resistance of the nitrided steel, revealing that it was notably more resistant than the untreated steel. Furthermore, it was observed that steel nitrided for shorter durations at lower temperatures (*e.g.*, 460°C for 4 h) demonstrated superior corrosion resistance compared to samples nitrided at higher temperatures.

Keywords: plasma nitriding, wear, corrosion, hardness, SEM and EDS

1 Introduction

The thermo chemical heat treatment procedure known as plasma nitriding also referred to as ion nitriding, pulse plasma nitriding, cold nitriding, or plasma hardening is used to improve the dependability and wear resistance of mechanically stressed metal components. Particularly mild surface treatment improves the materials' fatigue strength and corrosion resistance [1]. Nitrogen diffuses through the surface layer during plasma nitriding, causing a chemical change that generates nitrides with the treated material under the effect of heat [2]. As a result, surface hardness rises and wear resistance is much enhanced [3]. High-energy nitrogen, hydrogen, and their radicals bombard the cathode during plasma nitriding, causing nitrogen to chemisorb at the surface and diffuse into the metal to form the nitrided layer. Conventional methods of controlling and monitoring the process, such as monitoring temperature, gas composition, pressure, duty cycle, and visual observations of the nearby cathode regions to observe uniformity of the glow discharge, can also be used. Sputtering at the cathode/load surface and low nitrogen partial pressure lead to the formation of a very thin compound zone of iron nitrides, allowing us to identify plasma/ion nitriding as a low-nitriding potential process. Many different industries employ plasma nitriding, particularly for components that are exposed to high levels of stress, corrosion, and wear [4]. Numerous industries, including automotive, aerospace, and general engineering, use this low-temperature, low-distortion method [5]. The most recent surface hardening method for steel to extend its service life is plasma nitriding. A glow discharge technique using a combination of nitrogen and hydrogen gases is called plasma nitriding [6]. Diffused nitrogen on steel surfaces can include layers of FeN, Fe_3N, Fe_4N, and Fe_2N_3, with a micron size range of 10–100.

---

* **Corresponding author: C. Anil Kumar Reddy,** Department of Mechanical Engineering, Koneru Lakshmaiah Education Foundation, Vaddeswaram 522502, India, e-mail: anilreddymechanical@gmail.com
Pothamsetty Kasi V. Rao, Boggarapu Nageswara Rao: Department of Mechanical Engineering, Koneru Lakshmaiah Education Foundation, Vaddeswaram 522502, India
Begori Venkatesh: Mechanical Engineering, Vardhaman College of Engineering, Hyderabad 501218, India

Either some of the white/brittle layers can be removed, or the erosion/corrosion qualities can be strengthened [7]. It is clear from earlier research that nitrided layers subjected to friction and rolling contact fatigue are used for aircraft bearings. M50NiL steel must meet these requirements by having nitride layers with compound zones rather than an intergranular network of nitrides, which can only form in low nitriding potential. Additionally, this results in a shorter cycle time, regulated surface layer growth, the removal of the white layer, and less distortion [8]. High dimensional precision is ensured in this type of heat treatment since the samples are treated at substantially lower temperatures than in traditional hardening methods like carburizing and tempering [9]. Further cost savings can be achieved throughout the process chain thanks to plasma nitriding, since it eliminates the need for an expensive reworking of the specimens in the surface hardened condition or minimizes it [10].

1.1 Heat treatment

Plasma nitriding is a vacuum-supported surface treatment process renowned for its ability to enhance the properties of metallic work pieces or specimens [11]. Plasma nitriding is conducted at temperatures typically ranging from 260 to 600°C (500°F to over 1,112°F). Work pieces are first loaded into a vacuum chamber, where they function as the cathode and the furnace wall as the anode. An electric field is created between the charged work pieces and the furnace wall once the chamber is evacuated [3]. This electric field causes the treatment gas, typically nitrogen, to undergo ionization, forming a conductive gas known as plasma [12]. Within this plasma, nitrogen ions are accelerated toward the cathode (the work piece) under the influence of the electric current, resulting in high-energy collisions with the surface. Figure 2 provides a schematic representation of the plasma nitriding process, elucidating the intricate setup involved in this surface treatment technique [13].

The interaction between the accelerated nitrogen ions and the work piece surface results in several key phenomena [14]. First, the sputtering off of alien atoms cleans the surfaces finely, leaving a spotless surface ready for additional treatment. Additionally, passive layers present on materials like stainless steels or titanium are dissolved, enabling better adhesion and activation of the surface [15]. Simultaneously, the workpiece undergoes heating due to the energy transfer from the plasma, facilitating the diffusion of nitrogen into its surface [16]. This diffusion process is crucial for achieving the desired nitriding hardness depth, a parameter that determines the final properties of the treated workpiece [17].

Once the treatment temperature is reached, the holding time commences, during which the work pieces remain in the plasma environment for a duration dependent on material type and desired hardness depth [18]. With only roughly half the holding time needed for conventional gas nitriding techniques, plasma nitriding delivers substantial time savings. After the treatment cycle is over, the chamber is flooded with a gas to equalize pressure [19]. Subsequently, the work pieces undergo controlled cooling before they are removed from the chamber at low temperature [20].

The objective of this work is to increase the surface properties of M50NiL using plasma nitriding, which has demonstrated a notable increase in surface hardness and resistance. Previous research has shown that surface hardening techniques such as carburizing can achieve hardness levels up to 854 HV.

2 Experimental procedure

2.1 Material

A vacuum induction melting and VAR was used to manufacture the experimental M50NiL steel, which was then forged and heat-treated. A high-nickel, low-carbon variant of M50 steel is called M50NiL. It is also known as CBS-50NiL and AMS 6278 [21]. It is used for high temperature applications where surface strength and fatigue resistance are crucial. M50NiL's molybdenum content offers superior wear resistance, and its low carbon composition allows for outstanding toughness and it serves as alternative to M50 in high-temperature applications (up to 316°C) for components such as bearings, gears, *etc.* It is carburizable and nitriding able for wear resistance and fatigue strength, while its inner core maintains high fracture toughness [22]. Figure 1 depicts the chemical makeup of M50NiL steel. In

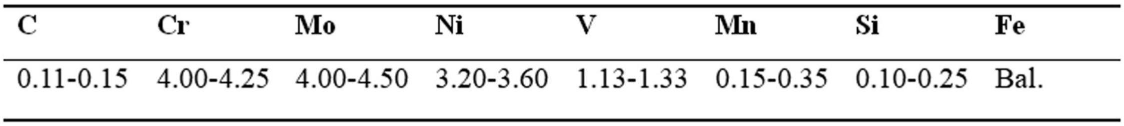

C	Cr	Mo	Ni	V	Mn	Si	Fe
0.11-0.15	4.00-4.25	4.00-4.50	3.20-3.60	1.13-1.33	0.15-0.35	0.10-0.25	Bal.

Figure 1: M50NiL steel composition (wt%).

the current study, M50NiL steel specimens of 10 mm × 10 mm × 5 mm were used. The samples were machined using EDM to measure 10 mm × 10 mm × 5 mm apiece from a 25 mm diameter rod. The samples' smooth surfaces were then polished using silicon carbide water-proof emery sheets to achieve grades 1,000 and 2,000 [23]. After polishing samples are cleaned with acetone. The samples are referred as PN460°C at 04 h to PN560°C at 40 h for nitriding treatment comprises 25 samples.

2.2 Plasma nitriding

The procedure was carried out using a large working volume (30 kW) plasma nitriding apparatus that was outfitted with the necessary heating and vacuum components (500 mm diameter × 500 mm height) as shown in Figure 2. The plasma was created by a pulsed DC power source operating at an average of 576 V. To empty the chamber to a base pressure of 5×10^{-2} mbar/pa, rotary pumps were used [24]. The samples were cleaned with argon and hydrogen gas at a 1:4 ratio and 1 mbar of pressure before plasma nitriding. The argon-hydrogen plasma removed the contaminants from the surface during the cleaning process [25]. The plasma nitriding process was carried out in the argon-nitrogen and nitrogen-hydrogen gas environments an hour later. The gas ratio (H_2:N_2) was 80:20, and the typical working pressure was 3–5 mbar.

The samples underwent plasma nitriding treatments at various temperatures and durations: 460°C for 4, 8, 12, 24, and 40 h; 500°C for 4, 8, 12, 24, and 40 h; 520°C for 4, 8, 12, 24, and 40 h; 550°C for 4, 8, 12, 24, and 40 h; and 560°C for 4, 8, 12, and 24 h. The treatments were conducted in a mixed gas atmosphere consisting of 80 H_2:20 N_2, at a constant pressure of 5 mbar, with current density of 1 (mA/cm^2). After the nitriding treatment, samples were slowly cooled inside the furnace chamber under a nitrogen atmosphere to prevent surface oxidation [26].

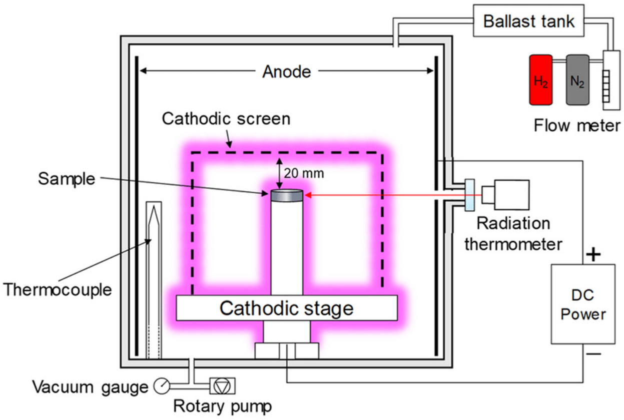

Figure 2: Plasma nitriding process [13].

2.3 Characterization

Mechanical characterization for untreated and plasma nitrided samples are conducted to identify microhardness; Vicker hardness tester Economet VH 1MD was used with load of 100 g and dwell period as 20 s. The changed layer's case depth was investigated using an optical microscope, the MET Scope-I, at magnifications of 100× and 500×. Using AQUAREGIA to etch the samples, the altered layer's depth was measured using an optical microscope. Scanning electron microscopy (SEM) and energy dispersive spectroscopy (EDS) are used to average two locations on the sample by Nova NanoSEM 450 apparatus and investigate the specimens' surface morphologies and element composition discrepancies.

Phase analysis of nitrided samples is performed by using with X-ray diffraction (XRD) method (BRUKER-D8 Advance) with Cu-Kα source and λ = 0.154093 nm wave length and for plasma nitrided samples. The diffraction patterns with a step size of 0.1° and a counting time of 2 s per step were achieved in the 2θ ranges of 20–120°. A pin-on-disc tribometer (TE-165-SPOD & Magnum Engineers) was used to assess the specimens' wear performance. The specimens (as a disc) were revolved for 1,800 s at a speed of 1,909 rpm, with a rotation of 3 mm (0.1 m/s), against a stationary M50NiL Sample of 10 mm × 10 mm. 20 N was the typical contact load. Every test was carried out in the open at a temperature of roughly 24°C. The wear rate (WR) was computed using the below formula [27]:

$$\text{Wear rate} = \frac{\text{Sliding distance}}{\text{Wear volume}},$$

$$\text{Specific wear rate} = \frac{\text{Wear volume}}{\text{Load} \times \text{Sliding distance}}.$$

Electrochemical corrosion studies are performed for plasma nitrided M50NiL samples on Biologic-SP 300 Potentiostat apparatus with 2 h 50 min and 30 min for Open circuit voltage (OCV), with scan rate of 0.2 mV/s from −1 V to +1 V. The samples are designated as PN460 at 04, 08, 12, 24, and 40 h and similarly for PN500, PN520, PN550, and PN560.

3 Results and discussion

3.1 Microstructure and phase structure analysis (XRD and SEM)

The phase structure in the nitrided surface was investigated using XRD (Bruker AXS, D8 Advance XRD system) with Cu-Kα radiation (λ = 0.15406 nm) in the range of angles 20–120° at the incidence angle of 0.1°, step size of 0.02°, and time per step of 2 s.

Figure 3(a) shows the X-ray patterns of the nitrided M50NiL samples. Based on XRD analysis, all the nitrided layers in the PN460 specimens are primarily composed of α-FeN, γ-FeN, and γ-Fe$_3$N. The α-FeN phase is dissolved in thePN460 at 40 h specimen. Adjusting the nitriding temperature is crucial for maximizing the wear and friction qualities since the compound layer greatly affects these parameters. Plasma nitriding at 500°C leads to the formation of various iron nitrides, with the extent of nitride formation increasing with the duration of nitriding. In Figure 3(b), the specimen PN500 at 40 h shows dissolved γ-FeN phase. This is explained by nitrogen being incorporated into the α-Fe lattice. Longer nitriding times lead to higher formation of γ-FeN and γ-Fe$_3$N, while the α-Fe content decreases. The evolution of these phases enhances the surface properties such as hardness and wear resistance, as nitrides are harder and more wear-resistant than pure iron. Plasma nitriding at 520°C induces the formation of iron nitrides, with the extent of nitride formation increasing with nitriding duration. The 24 h specimens at PN520°C exhibit the presence of α-Fe, as indicated by the XRD data in Figure 3(c). It is evident that the compound layer is primarily composed of γ-Fe$_3$N, γ-FeN, and α-FeN. The formation of these nitrides enhances surface hardness and wear resistance, as nitrides are harder and more wear-resistant than pure iron. The predominant phases found in the PN550 specimens are γ-FeN, γ-Fe$_3$N, and. Nevertheless, if the nitriding time is above 40 h, the α-FeN phase may emerge in the surface layer, signifying the completion of a phase structural change from Figure 3(d). The formation of these nitrides enhances surface hardness and wear resistance, as nitrides are harder and more wear-resistant than pure iron. The dynamic aspect of the nitriding process, which affects the treated material's microstructure and mechanical properties, is reflected in the variations in phase composition with nitriding time. XRD study of specimen PN560 at 40 h after plasma nitriding at 560°C shows the development of γ-Fe$_3$N and a small amount of γ-FeN phases (*i.e.*, the existence of γ-Fe$_3$N). The main components of the compound layer are γ-Fe and α-Fe$_3$N, with minute amounts of γ-Fe$_3$N remaining for up to 24 h and

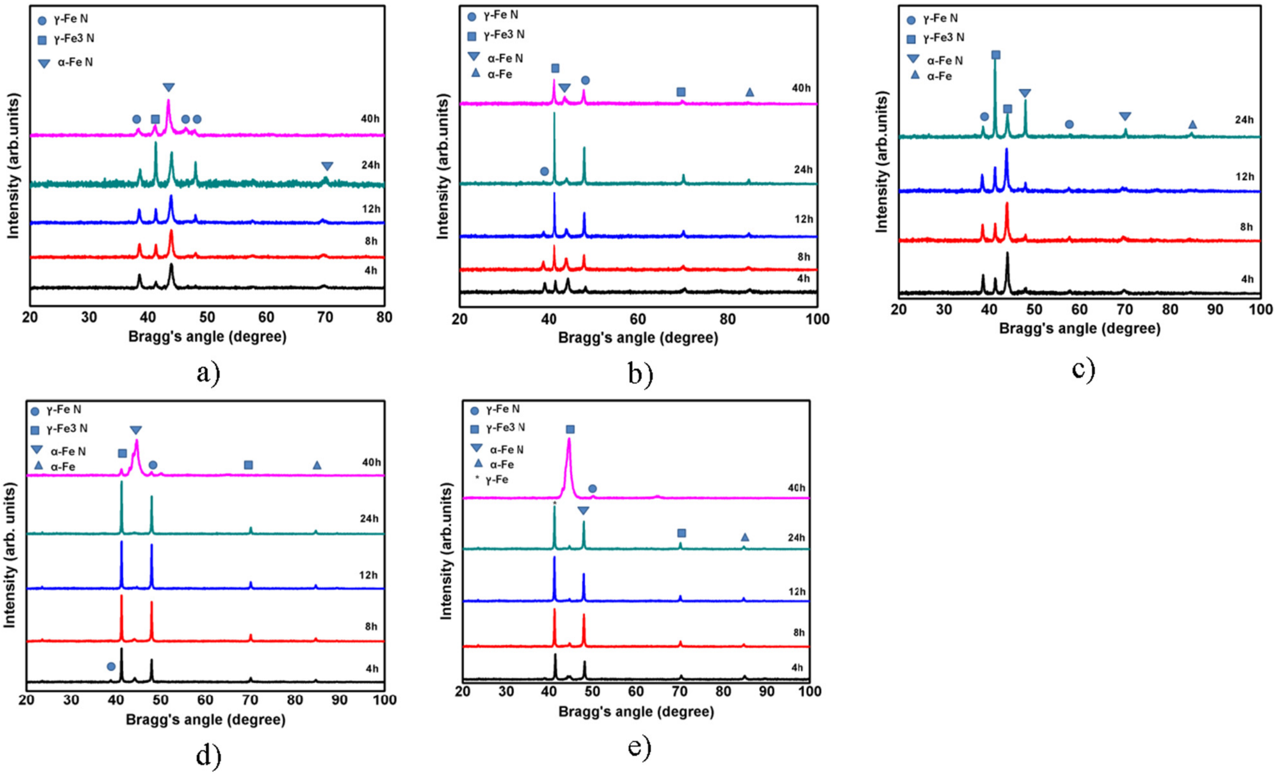

Figure 3: XRD profiles for plasma nitrided samples (460–560°C). Plots for (a) 460°C, (b) 500°C, (c) 520°C (d) 550°C, and (e) 560°C.

dissolving entirely after 40 h as shown in Figure 3(e). The formation of these nitrides enhances surface hardness, wear resistance, and corrosion resistance, while reduced friction and phase stability are maintained throughout the nitriding process.

The amount of nitrogen at the surface may decrease when nitriding temperature rises due to an increase in nitrogen diffusivity. The temperature of nitriding has no effect on the phase type of the compound layer. Changes in the temperature and nitriding time affect the peak intensity of the iron nitrides in the compound layer. Large size iron nitrides are more likely to develop in the compound layer during nitriding at high temperatures, as indicated by the fact that the peak intensity is highest at 520°C.

3.2 EDS analysis of plasma nitrided samples

EDS was conducted using an FEI NOVA 450 system attached to the SEM, enabling detailed chemical composition of a specimen. The nitrided M50NiL samples underwent EDS analysis to determine their chemical composition, with a specific focus on nitrogen content. EDS measurements were taken at random locations on the nitrided surface. The information produced by EDS analysis is in the form of spectra with peaks that represent the constituent components of the sample under examination. The EDS results for the plasma-nitrided layer of the M50NiL specimens are shown in Figure 4. The results were obtained after nitriding the specimens for different lengths of time (4, 8, 12, 24, and 40 h) at different temperatures (460, 500, 520, 550, and 560°C).

From Figure 4(a) and Table 1, the weight percentage of components found in EDS spectroscopy analysis for untreated M50NiL specimen is 9.9% C, 0.1% Al, 0.2% Si, 0.1% Ti, 1.1% V, 3.6% Cr, 0.3% Mn, 76.4% Fe, 0.9% Co, 2.8% Ni, 0.1% Cu, 4.2% Mo, and 0.4% W. EDS analysis at 460°C revealed that the PN460 at 40 h sample had a greater surface nitrogen content (4.7 wt%), while the PN460 at 12 h sample had a lower concentration (3.2 wt%). In addition, compared to the untreated sample, the carbon content for PN460 at 40 h dropped to 3.5 wt% as shown in Figure 4(b), most likely as a result of nitrogen atoms substituting carbon atoms during the nitriding process, which creates a nitride layer. At 500°C, the lowest nitrogen content was 8.6 wt% for the PN500 at 12 h sample, and the highest was 10.3 wt% for the PN500 at 08 h sample, which also contains high carbon content (11.6 wt%) in Figure 4(c). EDS detected less nitrogen of 7.2 wt% for PN520 at 12 h sample as shown in Figure 4(d) than the other samples nitrided at 520°C. The

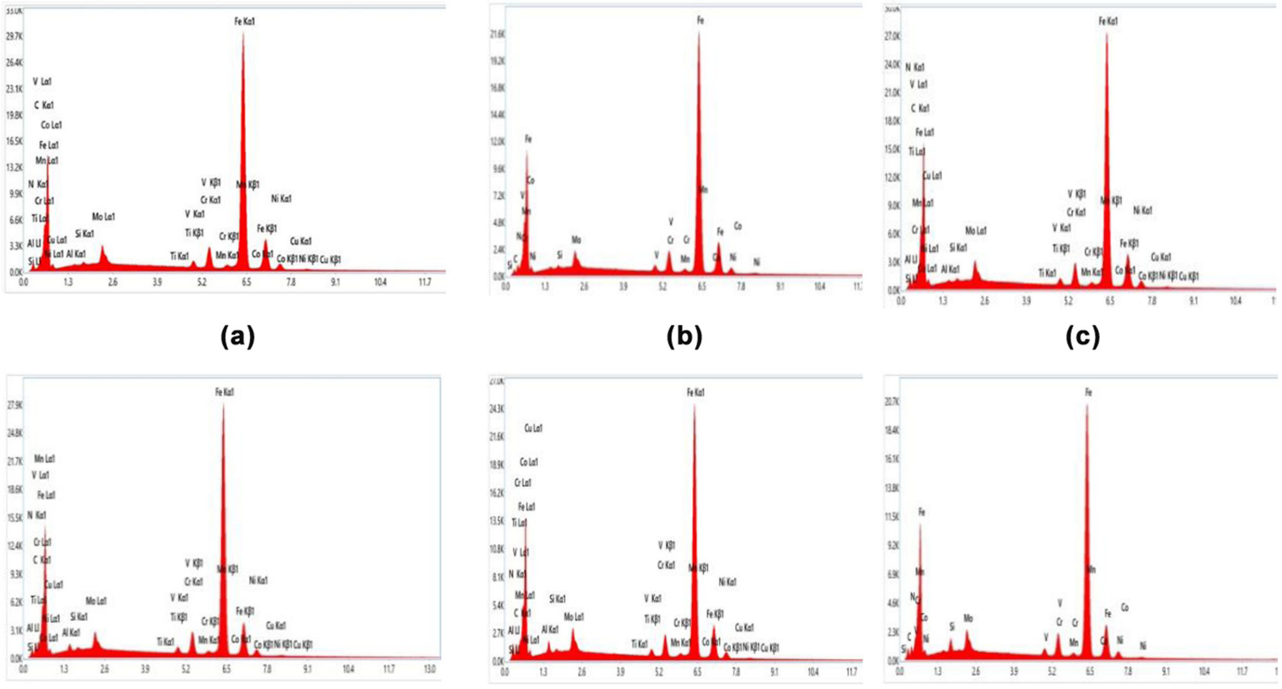
(a) (b) (c)

(d) (e) (f)

Figure 4: EDS analysis of plasma nitrided M50NiL specimens. (a) Untreated sample. (b) 460°C at 40 h. (c) 500°C at 08 h. (d) 520°C at 04 h. (e) 550°C at 24 h. (f) 560°C at 04 h.

Table 1: EDS analysis by SEM of nitrided M50NiL

Element (wt%)	Untreated	PN460°C at 40 h	PN500°C at 08 h	PN520°C at 04 h	PN550°C at 24 h	PN560°C at 04 h
Carbon (C)	9.9	3.5	11.6	7.3	14.9	11.9
Nitrogen (N)	0.0	4.7	10.3	9.7	12.0	9.7
Fluorine (F)	—	—		—	7.4	—
Aluminium (Al)	0.1	0.0	0.1	0.7	0.8	0.0
Silicon (Si)	0.2	0.2	0.2	0.2	0.1	1.0
Sulphur (S)	0.0	0.0	0.0	0.0	0.0	0.0
Titanium (Ti)	0.1	0.0	0.0	0.1	0.0	0.0
Vanadium (V)	1.1	1.0	0.9	1.0	0.8	0.9
Chromium (Cr)	3.6	3.7	3.1	3.3	2.5	3.1
Manganese (Mn)	0.3	0.3	0.3	0.4	0.3	0.3
Iron (Fe)	76.4	79.1	66.5	70.3	55.2	66.1
Cobalt (Co)	0.9	0.7	0.8	0.9	0.6	0.7
Nickel (Ni)	2.8	3.0	2.6	2.8	2.1	2.5
Copper (Cu)	0.1	0.0	0.1	0.1	0.1	0.0
Molybdenum (Mo)	4.2	3.8	3.4	3.3	3.2	3.8

PN520 at 04 h sample exhibits a nitrogen of 9.7 wt%, indicating a higher surface nitrogen concentration, and also shows a carbon content of 7.3 wt%. At 550°C as shown in Figure 4(e), the PN550°C at 40 h specimen, when subjected to a longer nitriding duration of 40 h, shows lower nitrogen content (3.1 wt%) and higher carbon content of 21 wt% and the 24 h nitrided sample (PN550 at 24 h)exhibits a higher nitrogen content of 12 wt%, alongside a carbon content of 14.9 wt% and also iron content is 55.2 wt%, which is lower than the untreated sample (76.4 wt%).The nitrogen content in the nitrided sample PN560 at 04 h is 9.7 wt%, accompanied by 11.9 wt% carbon and 66.1 wt% iron. In contrast, when treated at 560°C, the PN560 at 08 h sample exhibits a low nitrogen content of 5.2 wt% as shown in Figure 4(f).

Even though the EDS measurements were made at random locations on the M50NiL steel surface, it is clear from the EDS analysis results that the steel's nitrogen concentration rises with the length of solution nitriding. The sample taken at 40 h had the lowest nitrogen level (4.7 wt %), whereas the sample taken at 24 h had the highest nitrogen amount (12.0 wt%). This suggests that a longer nitriding time generally permits more nitrogen to diffuse into the steel at lower temperatures. On the other hand, shorter or moderate nitriding times are adequate for efficient nitrogen uptake at higher temperatures.

3.3 Microstructure of plasma nitrided layers

Using an EDS equipment in conjunction with a SEM (FEI NOVA 450/650), the cross-sectional microstructure, surface morphologies, and elemental distributions were observed.

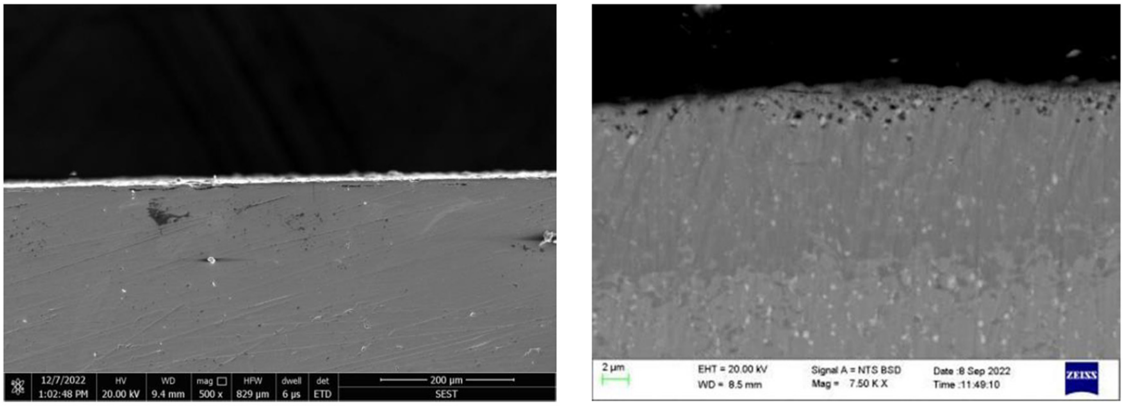

(a) **(b)**

Figure 5: SEM micrograph of the plasma nitride steel (460–560°C). (a) Microstructure for 460°C at 40 h. (b) Microstructure for 520°C at 40 h.

Figure 5a provides a SEM image of a sample that was nitrided at 460°C for 40 h, providing information about the precise structure of the compound layer that formed at the surface during the nitriding process. It is evident that the nitrided layer is made up of a diffusion layer with a specific thickness underneath and a compound layer on top. The dazzling white layer on the surface is a direct result of nitrogen diffusing into the steel during plasma nitriding, as Figure 5 makes abundantly evident. Nitrides, which are hard chemicals that improve surface hardness and wear resistance, make up this layer.

There is a clear, defined separation between the substrate and the nitrided layer, which suggests that nitrogen has been carefully injected into the steel. Effective and reliable nitriding conditions are suggested by the homogeneity of the nitrided layer. The little flaws that were noticed might be the result of intrinsic material imperfections or gas entrapment. Under a microscope, the α-FeN particles have a bright colour.

The SEM micrograph displays a bright, continuous layer on the surface of the M50NiL steel, which represents the nitrided layer formed during the plasma nitriding process at 520°C for 40 h (from Figure 5(b)). The depth of this nitrided layer appears to be around 5–6 µm. The darker region below the nitrided layer is the substrate of M50NiL steel. This area retains its typical microstructure, likely composed of fine-grained martensite and retained austenite, as is characteristic of high-performance bearing steels. The interface between the nitrided layer and the substrate, while still sharp, shows evidence of deeper diffusion. The substrate retains its original microstructure of fine-grained martensite and retained austenite, crucial for maintaining the steel's toughness and strength. The cross-section micrographs show that thicker case depths occur as a result of increasing process temperature, which also increases nitrogen diffusivity.

3.4 Surface mechanical properties (hardness and corrosion, wear)

3.4.1 Micro hardness

A Vickers micro hardness tester (ECONOMET VH 1MD) was used to measure the micro hardness profiles of the nitrided layers for 10 s while subjected to a 100 g load. To ensure measurement accuracy, the mean value of three indentations produced at the same depth into the nitrided layer was used.

Figure 6 displays the micro hardness profile of nitrided samples with temperature and nitriding soaking time ranging from 4 to 40 h, respectively. Since the nitrided M50NiL steel has a surface micro hardness of more than 1,000 HV, plasma nitriding can greatly boost the surface micro hardness. The hardness of raw M50NiL specimen is approximately 297.5 HV. When nitrided at 460°C, a maximum hardness of approximately 1,150 HV is observed after 40 h. This is likely due to the prolonged diffusion of nitrogen atoms into the material, resulting in deeper nitriding and increased hardening. The hardness profile shows a maximum hardness of approximately 1,333 HV at 500°C for 4 h, possibly influenced by the presence of large primary carbides during the measurement, which could have affected the result. At 520°C, the specimen PN520 at 12 h achieves a peak hardness of around 1,278 HV. At 550°C, after nitriding for a longer duration of 40 h, the hardness peaks at around 1,085 HV. This is potentially due to the formation of harder nitride phases or the increased depth of the nitrided layer. At 560°C, the maximum hardness is approximately 1,045 HV for 12 h of nitriding, decreasing to around 1,004 HV after 40 h. The decrease in hardness at higher temperatures and longer durations could be due to over-aging or coarsening of nitride precipitates, leading to reduced strengthening effects. The hardness of nitrided specimens decreases with increasing nitriding temperature (from 500°C), indicating that hardness is a function of treatment temperature. The nitriding process functions similar to the tempering process due to the decrease in carbon saturation in the α-Fe phase: the lower the core hardness, the higher the treatment temperature. However, the corresponding case depths of the nitrided samples thicken with increasing temperature.

The results show that specimen PN560 has a lower micro hardness of 1,004 HV 0.1 at 40 h when the

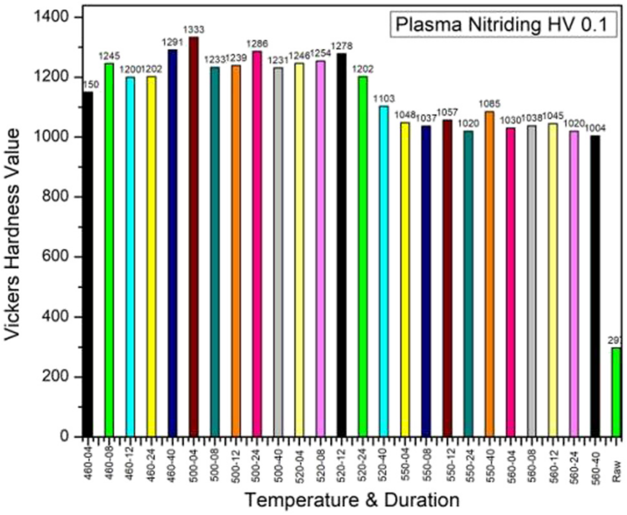

Figure 6: Hardness values for plasma nitrided specimens.

temperature during nitriding is higher than 500°C, *i.e.*, 560°C. This drop in hardness is probably caused by the ferrite phase being less dense at higher heat treatment temperatures. Compared to other specimens, the PN500 at 04 h specimen has a greater micro hardness profile in the surface layer. After nitriding the sample for 40 h at 560°C, the maximum thickness of the nitride layer was measured at 354.00 µm.

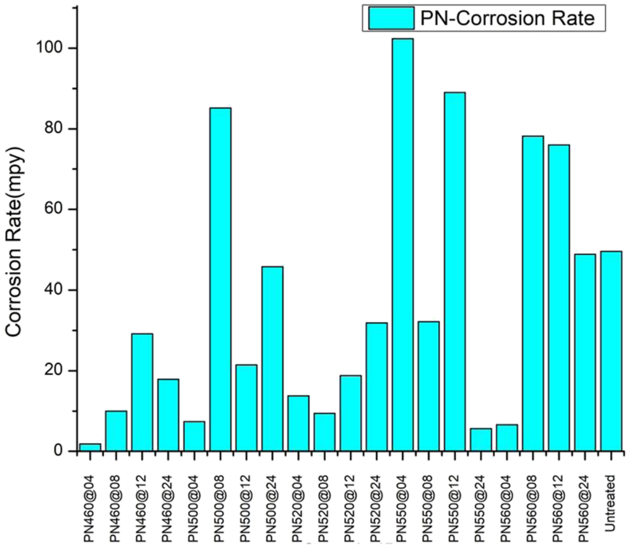

Figure 8: Corrosion rate for plasma nitrided samples and untreated samples.

3.4.2 Corrosion behaviour

Electrochemical tests were conducted in a 3.5 wt% NaCl electrolyte solution using a Biologic SP300 potentiostat controlled by EC Lab software, running at a scan rate of 0.5 mV/s to generate potentiodynamic anodic and cathodic polarization curves.

Potentiodynamic polarization graphs of the plasma-nitrided specimens and untreated M50NiL steel are displayed in Figure 7(a–e). The corrosion parameters Ecorr, Icorr, and corrosion rate were computed from the Tafel plots (Tp) and are shown in Figure 8. It is clear that the nitrided specimen's corrosion potential shifts in the direction of the anode. It suggests that the corrosion reaction's thermodynamic trend beneath the system is waning. The results show that nitriding at a low temperature of 460°C can significantly increase corrosion resistance and that samples treated at this temperature exhibit the best corrosion behaviour. It was discovered that Icorr and the corrosion rate for the nitrided steels were substantially lower than those of the untreated steel. The corrosion current density (Icorr) of untreated specimen is 108.221 µA, while

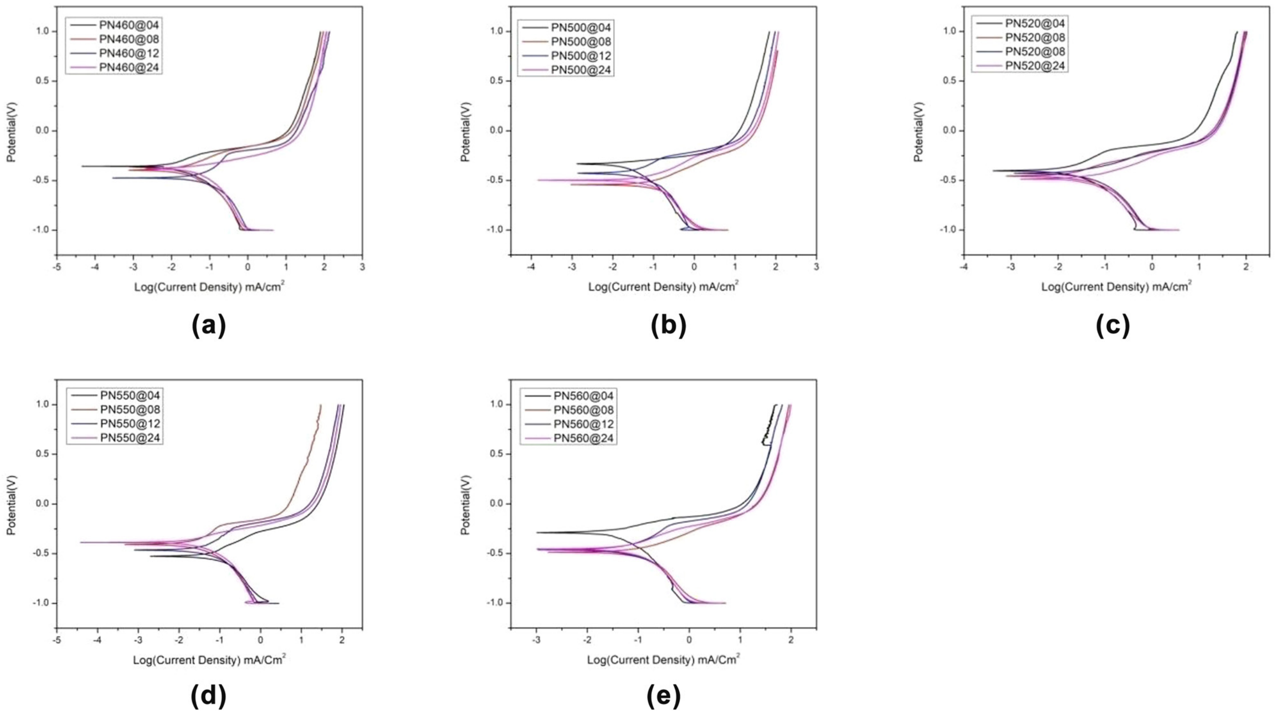

Figure 7: Tp of plasma nitrided samples at 460, 500, 520, 550, and 560°C for 4, 8, 12, and 24 h respectively. (a) Tp at 460°C. (b) Tp at 500°C. (c) Tp at 520°C. (d) Tp at 550°C. (e) Tp at 560°C.

those of nitrided specimens are lower. Nitrided samples have better corrosion resistance than untreated samples. Nitrided specimens exhibit higher anti-solubility during anodic dissolution, as indicated by their lower polarization current density at the same anode electrode potential.

When nitrided at 460°C for 4 h, the specimen showed a corrosion rate of 1.80403 mpy, significantly lower than the untreated sample's rate of 49.577 mpy as shown in Figure 7(a). Among the nitrided samples, PN460 at 04 h exhibited the best corrosion performance, with a corrosion current (I_{corr}) of 3.938 µA, notably lower than the other samples. The nitrided sample PN460°C at 04 h showed more positive zero current (E_{corr}) of −357.472 mV than the untreated material. In Figure 7(b), PN500°C at 04 h demonstrates a corrosion rate of 7.38333 mpy, indicating its resilience to corrosion in test conditions. Figure 7(c) depicts PN520 at 08 h exhibits a corrosion rate of 9.41596 mpy, highlighting its durability in harsh environments. PN550 at 24 h shows a corrosion rate of 5.59992 mpy as shown in Figure 7(d), showcasing its excellent resistance even under prolonged exposure. In Figure 7(e), PN560 at 04 h exhibits a corrosion rate of 6.56882 mpy, indicating strong resistance, especially under high temperature and short duration conditions. And with an OCV reading of −0.30, the nitrided steel 560 at 04 h exhibits a less noble corrosion potential indicative of enhanced corrosion resistance. PN550 at 04 h shows significantly higher anodic kinetics, with a corrosion current density (Icorr) of 223.386 µA. This sample displayed the highest corrosion rate among the group, at 102.335 mpy, suggesting that plasma nitriding at this condition may be less effective, possibly due to increased nitrogen diffusion leading to brittleness.

3.5 Tribological performance (wear and Coefficient of Friction, COF)

The pin-on-disc wear tests were carried out at a constant load of 20 N and a sliding velocity of 1.0 m/s with a constant sliding distance of 3,600 m keeping other parameters constant and the COF results are presented in Figure 9(a–e) and WR in 9 (f).

The untreated and nitrided M50NiL steel specimens tested against a tungsten carbide ball for 3,600 s under a load of 20 N are shown in Figure 9 along with their respective friction coefficients and WRs. The high hardness of the nitrides on the changed surface gives the nitrided samples nearly the same friction coefficients. Compared to the nitrided specimens, the untreated specimen has a higher friction coefficient of 0.5773. This suggests that the creation of a nitrided layer improves frictional characteristics in

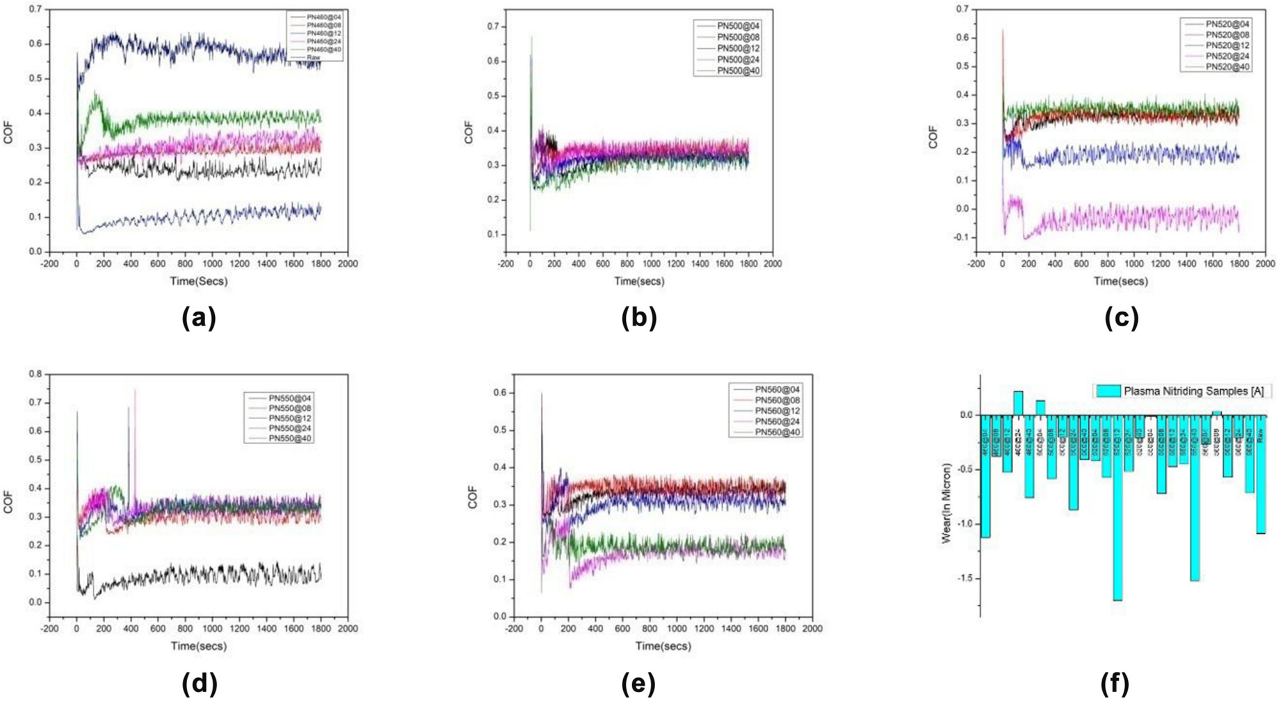

(a) (b) (c)

(d) (e) (f)

Figure 9: COF of the specimens treated at 4, 8, 12, 24, and 40 h for temperatures (a) 460°C, (b) 500°C, (c) 520°C, (d) 550°C, and (e) 560°C; (f) WR of untreated and nitrided samples.

addition to surface hardness. Figure 9 shows that the friction coefficient of the PN460 at 12-h specimen is 0.1001, which is less than that of the other samples. The nitrided samples' friction coefficients are initially lower than those of the untreated sample, but they eventually rise to a stable condition. The nitrided samples (*i.e.*, 460–560°C) have friction coefficients of around 0.3095, 0.3230, 0.3492, 0.3029, and 0.3438 for the 460 at 24 h, 500 at 04 h, 520 at 40 h, 550 at 04 h, and 560 at 08 h, respectively, in the stable state. The nitrided samples exhibit an increase in friction coefficient in relation to both treatment time and temperature. At 40 h, the PN520°C sample exhibits greater friction coefficients when subjected to a 20 N load. The volume WRs of the specimens were found and computed using the provided formula in order to better characterize the wear parameters of the untreated and plasma nitrided specimens. The findings are displayed in Figure 9(f).

With a friction coefficient of 0.3095 and a WR of 0.38 × 10^{-6} g/m (0.22050 microns), the PN460 at 24 h sample exhibits the lowest WR, whereas the untreated sample has a WR of 0.36 × 10^{-6} g/m (−0.71258). The PN460°C at 24 h specimen's surface structures show that the ε-$Fe_{2-3}N$ phase's hexagonal close-packed structure – which has more atomic binding forces and fewer slip systems – improves wear resistance. As a result, the 24 h sample of PN460 had the highest wear resistance and the lowest WR. With a friction coefficient of 0.1915 and high wear of 0.83 × 10^{-6} g/m (−1.70183), the PN520 sample at 12 h shows less resistance to wear than the other nitrided samples.

At 500°C, the PN500 at 04 h sample demonstrates a low WR of 0.05 × 10^{-6} g/m (0.13475), highlighting its superior wear resistance and 0.3230 as COF. Among the specimens nitrided at 520°C, the one with the most pronounced wear resistance is the sample (PN520 at 40 h) treated for 40 h, indicated by its low WR value of 0.11 × 10^{-6} g/m (−0.20377) with COF of 0.3492. The reason could be attributed to the presence of thick nitride layer comprising of hard nitrides resulting from prolonged nitriding at the surface. The PN550 at 04 h sample has shown a low WR of 0.25 × 10^{-6} g/m (−0.00546) with 0.3029, which indicates excellent wear resistance compared to other samples treated at 550°C. The PN560 at 08 h sample has 0.3438 COF and showed a low WR of 0.13 × 10^{-6} g/m (0.03553) than the other samples nitrided at 560°C.

Figure 9(f) plots the WR of the untreated material and the sample nitrided at different temperatures. It demonstrates how raising the processing temperature reduces WR.

The wear volume of the plasma nitrided specimens 460 at 24 h, 500 at 04 h, 520 at 40 h, 550 at 04 h, and 560 at 08 h for an applied load of 20 N with a sliding speed of 1,909 rpm were found to be 0.143 × 10^{-3}, 0.016 × 10^{-3}, 0.045 × 10^{-3}, 0.116 × 10^{-3}, and 0.069 × 10^{-3} mm^3/m for a sliding distance of 3,600 m, respectively.

4 Conclusion

M50NiL steel specimens with different temperatures ranging from 460 to 560 with a duration of 4, 8, 12, 24, and 40 h are investigated to identify the phase structure, micro structural changes, wear, corrosion, and micro hardness. In future, this entire work can be optimized according to process parameters to obtain best operational conditions and from above observations the major outcomes are as follows:

(a) The plasma nitride layer includes diffusion layer and after nitriding, α-FeN and γ-FeN as well as γ-Fe_3N phases are formed on the M50NiL surface layer.

(b) Microhardness of plasma nitrided M50 NiL samples at 500°C for 4 h is 1,333 HV which is six times more than the untreated sample is 294 HV, possibly influenced by the presence of large primary carbides during the measurement.

(c) The wear resistance and friction coefficient of M50NiL plasma nitride samples at 500°C at 04 h sample shows the lowest WR of 0.05 × 10^{-6} g/m and a friction coefficient of 0.3230 whereas the untreated sample has a WR of 0.52 × 10^{-6} g/m with 0.5773 as COF. The friction coefficient and WR of the nitrided specimens are lower than the untreated samples.

(d) Corrosion resistance behaviour of M50NiL nitride sample is significantly improved for 460°C at 4 h, the specimen showed a corrosion rate of 1.804 mpy, significantly lower than the untreated sample's rate of 49.577 mpy.

Funding information: This work was funded by Aeronautical Research and Development Board (ARDB), New Delhi Under research grant (1957). The authors acknowledge the support of ARDB for this article.

Author contributions: All authors have accepted responsibility for the entire content of this manuscript and consented to its submission to the journal, reviewed all the results, and approved the final version of the manuscript. B.V. and P.K.V.R. designed the experiments and C.A.K.R. carried them out. B.N.R. developed the model for characterization. C.A.K.R. prepared the manuscript with guidance from all co-authors.

Conflict of interest: Authors state no conflict of interest.

Ethical approval: The conducted research is not related to either human or animals use.

Data availability statement: Data sharing is not applicable to this article as no datasets were generated or analysed during the current study.

References

[1] Trinadh K, Nouveau C, Rao KRM. Effects of plasma nitriding on low alloy Cr-Mo-V steel. Mater Today: Proc. 2021;40:S79–82.
[2] Wang X, Yan MF, Zhang CS, Zhang YX, Bai B, Chen L, et al. Insights into plasma nitriding behaviour of M50NiL steel with different initial microstructures. Mater Sci Technol. 2013;30(10):1248–53.
[3] Díaz-Guillén J, Naeem M, Acevedo-Davila J, Hdz-Garcia H, Iqbal J, Khan M, et al. Improved mechanical properties, wear and corrosion resistance of 316L steel by homogeneous chromium nitride layer synthesis using plasma nitriding. J Mater Eng Perform. 2020;29:877–89.
[4] Jin J, Chen YB, Gao KW, Huang XL. A study of the corrosion resistance of M50NiL bearing steel by ion implantation. Adv Mater Res. 2014;936:1132–7.
[5] Karakan M, Alsaran A, Çelik A. Effects of various gas mixtures on plasma nitriding behavior of AISI 5140 steel. Mater Charact. 2002;49(3):241–6.
[6] Was GS, Demaree JD, Rotberg V, Kim K. Corrosion and mechanical behavior of ion implanted bearing steels for improved fretting behavior. Surf Coat Technol. 1994;66(1–3):446–52.
[7] Mann BS, Arya V. An experimental study to correlate water jet impingement erosion resistance and properties of metallic materials and coatings. Wear. 2002;253(5–6):650–61.
[8] Erdemir A, Hochman RF. Corrosion behavior of TiN ion plated M-50 bearing steel. J Mater Energy Syst. 1985;7(3):265–8.
[9] Wang F, Zhou C, Zheng L, Zhang H. Corrosion resistance of carbon ion-implanted M50NiL aerospace bearing steel. Prog Nat Sci Mater Int. 2017;27(5):615–21.
[10] Wang F, Zhou C, Zheng L, Zhang H. Improvement of the corrosion and tribological properties of CSS-42L aerospace bearing steel using carbon ion implantation. Appl Surf Sci. 2017;392:305–11.
[11] Nielsen BR, Torp B, Rangel CM, Simplicio MH, Consiglieri AC, DaSilva MF, et al. Improvement of corrosion resistance of M50 bearing steel by implantation with metal ions. Nucl Instrum Methods Phys Res Sect B Beam Interact Mater At. 1991;59–60:772–7.
[12] Trinadh K, Nouveau C, Khanna AS, Aneja KS, Rao KRM. Electrochemical study on the corrosion resistance of surface modified Cr-Mo-V steel by elevated temperature plasma nitriding. Mater Res Express. 2019;6(7):076507.
[13] Karimoto T, Nishimoto A. Plasma-nitriding properties of CoCrFeMnNi high-entropy alloys produced by spark plasma sintering. Metals. 2020;10(6):761.
[14] Yan MF, Wang XA, Liu RL, Zhang YX, Yang Y. Kinetics and wear behaviour of M50NiL steel plasma nitrided at low temperature. Mater Sci Technol. 2016;33(3):370–6.
[15] Wang X, Yan M, Liu R, Zhang Y. Effect of rare earth addition on microstructure and corrosion behavior of plasma nitrocarburized M50NiL steel. J Rare Earths. 2016 Nov;34(11):1148–55.
[16] Menthe E, Bulak A, Olfe J, Zimmermann A, Rie KT. Improvement of the mechanical properties of austenitic stainless steel after plasma nitriding. Surf Coat Technol. 2000 Nov;133–134:259–63.
[17] Shi J, Gao MZ, Wang TM, Wen XY, Shi WD. Corrosion wear behaviour of ion-implanted steel. Wear. 1994;176(2):145–9.
[18] Wang XA, Yan MF, Zhang CS, Zhang YX. Microstructure and mechanical properties of surface layer of M50NiL steel plasma nitrided. Surf Eng. 2014;30(3):218–3.
[19] Zhang CS, Yan MF, Sun Z, Wang YX, You Y, Bai B, et al. Optimizing the mechanical properties of M50NiL steel by plasma nitrocarburizing. Appl Surf Sci. 2014;315:28–35.
[20] Larisch B, Brusky U, Spies HJ. Plasma nitriding of stainless steels at low temperatures. Surf Coat Technol. 1999;116–119:205–11.
[21] Tang LN, Yan MF. Influence of plasma nitriding on the microstructure, wear, and corrosion properties of quenched 30CrMnSiA steel. J Mater Eng Perform. 2013;22(7):2121–9.
[22] Basu A, Majumdar JD, Alphonsa J, Mukherjee S, Manna I. Corrosion resistance improvement of high carbon low alloy steel by plasma nitriding. Mater Lett. 2008;62(17–18):3117–20.
[23] De Almeida EA, Da Costa CE, Milan JC. Study of the nitrided layer obtained by different nitriding methods. Matéria (Rio De Janeiro). 2015 Jun;20(2):460–5.
[24] Kumar A, Kaur M, Joseph A, Jhala G. Surface engineering analysis of plasma-nitrided die steels. Proc Inst Mech Eng Part J J Eng Tribol. 2019;234(6):917–31.
[25] Roliński E. Plasma nitriding process and best applications. Heat Treat 2023: Proceedings of the 32nd ASM Heat Treating Society Conference; 2023. p. 77–81.
[26] Miyamoto J, Abraha P. The effect of plasma nitriding treatment time on the tribological properties of the AISI H13 tool steel. Surf Coat Technol. 2019;375:15–21.
[27] Roliński E. Plasma-assisted nitriding and nitrocarburizing of steel and other ferrous alloys. In: Mittemeijer EJ, Somers MAJ, editors. Thermochemical surface engineering of steels. London: E-Publishing Inc.; 2015. p. 413–57.